Understanding the Correlation Between Intermetallic Growth, Stress Evolution, and Sn Whisker Nucleation

Nitin Jadhav, Eric J. Buchovecky, Lucine Reinbold, Sharvan Kumar, Allan F. Bower, and Eric Chason

***Abstract*—Stress due to intermetallic (IMC) growth is generally accepted as the driving force for Sn whisker formation, but there are still many unanswered questions regarding the development of stress and how it relates to the growth of whiskers. We have made simultaneous measurements of the evolution of stress, IMC volume, and whisker density on samples of different thicknesses to address the underlying mechanisms of whisker formation. Finite-element simulations are used to study the stress evolution due to IMC growth with various stress relaxation mechanisms: plastic deformation coupled with grain boundary diffusion is found to explain observed stress levels, even in the absence of whisker growth. A model of whisker growth suggests that the average steady-state stress is determined primarily by relaxation processes (dislocation- and diffusion-mediated) and that whisker growth is not the primary stress relaxation mechanism. Implications of our results for whisker mitigation strategies are discussed.**

***Index Terms*—Electronics packaging, lead free, Sn whiskers, tin, tin alloys, whisker density.**

I. Introduction

Sn-based coatings are used extensively as protective coatings on Cu conductors in electronics manufacturing. The migration to Pb-free processing has created problems related to whisker formation: thin filaments of Sn are found to grow out of the coatings and can induce short circuits. Although the problem is widely recognized, a comprehensive understanding of whisker formation has still not been developed. The problem is complicated by the fact that the microstructure of the system is complex, and many competing kinetic processes play a role. In addition, many factors have been shown to influence whisker formation, making it difficult to compare results from one system with measurements from another.

The driving force for whisker formation is generally accepted to be stress generated by the formation of Cu_6Sn_5 intermetallic (IMC) between the Sn and Cu. However, many of the underlying processes controlling whisker formation are not understood. Outstanding questions include: how is the stress generated in the Sn, and how does it spread throughout the Sn layer? How does the stress depend on IMC growth kinetics? What are the mechanisms for relaxing stress in the Sn film? How does stress lead to whisker formation? A greater fundamental understanding of these issues is needed to develop reliable mitigation strategies as well as to develop models to predict whisker formation.

To answer these questions, we need systematic studies to probe the driving forces and kinetic processes that control whisker formation and growth under different conditions. Therefore, we have measured the kinetics of IMC formation, stress evolution, and whisker density evolution with time on a series of identically grown samples with different Sn layer thicknesses and grain sizes. Because the measurements are performed simultaneously in real-time, we have been able to directly observe the correlation among these different parameters. As described below, we find that thicker, larger-grained films have greater rates of IMC growth, yet the resulting stress is reduced. In addition, the number of whiskers per unit area is reduced.

To relate these measurements to underlying physical mechanisms, we have used finite-element analysis (FEA) to simulate stress evolution due to IMC growth in a film which relaxes by different mechanisms including dislocation motion and grain boundary diffusion. These simulations predict stress levels that are in excellent agreement with experiment, and provide insight into how the stress spreads throughout the Sn layer in response to the IMC growth. We also describe a simple FEA model of whisker growth in a stressed film that was developed to address how and why whiskers might form. The model shows that any microstructural feature that tends to reduce the stress in one grain relative to the rest of the film will generate a local stress gradient around that grain. Even though the average stress in the film may be low due to relaxation processes, large stress gradients can develop locally around the whisker, and are maintained by continued growth of IMC in the film. These gradients provide the driving force for material to diffuse towards the whisker root where it can be incorporated into the whisker and removed as the whisker grows out of the film. The model is found to predict whisker growth rates that are in good agreement with experiment.

The remainder of this paper is organized as follows. In the next section, we briefly summarize current understanding of the mechanisms for stress generation and whisker formation in Sn films. We then describe in detail our experimental procedure for simultaneously measuring stress, IMC volume, and whisker density, and describe the results of these experiments. Finally, we discuss the implications of the experimental results on IMC growth kinetics, stress generation and relaxation, and whisker

Manuscript received July 01, 2009; revised December 03, 2009. This work was supported in part by the Brown MRSEC under Grant DMR0079964, in part by the National Science Foundation (NSF) under Grant DMR0856229, and in part by the EMC^2 Corporation. This work was recommended for publication by Associate Editor R. Gedney upon evaluation of the reviewers comments.

N. Jadhav, E. J. Buchovecky, S. Kumar, A. F. Bower, and E. Chason are with the Division of Engineering, Brown University, Providence, RI 02912 USA (e-mail: nitin_jadhav@brown.edu).

L. Reinbold is with the Maritime Mission Center, Raytheon Company IDS, Portsmouth, RI 02871 USA.

Color versions of one or more of the figures in this paper are available online at http://ieeexplore.ieee.org.

Digital Object Identifier 10.1109/TEPM.2010.2043847

nucleation and growth. Our finite-element simulations and results are included with this discussion.

II. Background

Whisker growth on Sn-plated electronic components has been documented since the 1940s [1]–[4] and many studies have subsequently been performed [5]. We do not try to summarize the large literature on Sn whisker studies, but instead merely note some important insights from others that are relevant to the work described here. A large number of mechanisms have been proposed to explain the formation of whiskers, including recrystallization [6]–[10], oxidation [2], [11], [12], and stress [13]–[32]. The general consensus is that stress is the most likely driving force for whisker nucleation and growth. There are many possible sources of stress, including an externally applied force [22]–[24], residual stress from deposition or thermal expansion mismatch, or IMC formation between the Sn and Cu. Of these, only stress due to IMC growth can continue to increase with time after the initial deposition process.

Development of internal stress in the layers has been reported in multiple studies [14], [16], [26], [30], [33]. Lee and Lee [13] measured compressive stress in the Sn layer using a beam deflection method and proposed that the stress develops as a consequence of IMC formation within Sn grain boundaries near the Cu–Sn interface. Choi *et al.* [19] utilized micro-diffractometry via synchrotron radiation to show that the stress is highly inhomogeneous and varies from grain to grain (the stress is biaxial only when averaged over several grains). Similarly, recent work by Sobiech *et al.* [34] indicates stress gradients around the whisker root. Boettinger *et al.* [18] used beam deflection to compare stress evolution and whisker formation on Sn, Sn–Cu, and Sn–Pb electrodeposited layers. Their results point to the importance of the layer composition in affecting the growth of the intermetallic particles and altering the stress state.

The kinetics of the IMC growth process was studied by Tu and coworkers using X-ray diffraction (XRD) [14] and Rutherford backscattering spectroscopy (RBS) [35]. Marker experiments indicated that Cu is the dominant diffusing species. Other investigators have determined the kinetics of intermetallic growth by measuring the weight change when the Sn layer is chemically stripped from the Sn–Cu film structure [17], [36] after various times. Zhang *et al.* [17] correlated the intermetallic volume with the morphology of particles at the interface using atomic force microscopy (AFM).

Whisker growth is generally viewed as a mechanism for relaxing compressive stress in the Sn by transporting material out of the plane of the film. Given that whiskers typically attain lengths many times greater than the thickness of the film and the film immediately surrounding a whisker does not show signs of obvious thinning, it is widely assumed that long-range transport is necessary to supply sufficient material to the whisker to sustain growth [22], [37]. At room temperature, the dominant pathway for long-range diffusion of Sn atoms is along the Sn–Sn grain boundaries as indicated by tracer diffusion studies [38].

Tu [39] suggested that whisker growth occurred by long-range diffusion of Sn atoms to relieve compressive stress generated by the formation of the IMC, and developed an analytical model relating whisker growth kinetics to the Sn stress. Lee and Lee [13] and Tu *et al.* [40] also pointed out the importance of cracking the oxide to initiate whisker growth. Smetana [41] has written about the grain structure needed around the base of the whisker to enable it to crack the oxide and relieve stress.

TABLE I
Measured Grain Size in Sn Layers of Different Thicknesses

Sn layer thickness (nm)	Grain size (μm)
1450	1.42
2900	1.92
5800	3.22

In spite of the extensive number of studies, it is difficult to make generalizations because of the wide variety in growth conditions, film thickness, microstructures, and other important parameters used in different works. For this reason, we have tried to measure several parameters (IMC volume, stress, whisker density) simultaneously on well-characterized samples with different layer thicknesses (Table I) to enable us to understand the relationship between them.

III. Experiment

The samples consisted of electrodeposited Sn layers grown over Cu layers that had been vapor-deposited on oxidized Si substrates. This structure enabled us to control the microstructure and cleanliness of the layers and provided a suitable structure for making wafer curvature measurements of stress. The Sn layers were grown using a commercial Sn plating solution in a three-electrode cell controlled by a potentiostat with a SCE (Saturated Calomel) reference electrode. The substrates were (100)-oriented silicon single crystals with a 100-nm-thick SiO_2 layer; the substrates were 200 μm thick in the form of 25.4 mm $\times$ 12.5 mm rectangles. The substrates were initially coated with a 15-nm Ti seed layer (for better adhesion) followed by 600 nm of Cu in a Temescal electron-beam evaporator under a vacuum of 4.0×10^{-4} Pa. The Sn was electrodeposited at a constant current density of 10 mill-amps/cm^2 over the copper layer after removal from the vacuum system. In order to remove the copper oxide layer (which might have formed as we expose the Cu coated sample to atmosphere), the sample was dipped in sulphuric acid for 10 seconds and was rinse twice in DI water for 60 seconds before Sn electrodepositionThe resulting Sn microstructure consists of columnar grains with predominantly vertical grain boundaries, which is typical of Sn platings [18], [42], [43].

This procedure was used to prepare sets of samples with three different thicknesses of Sn: 1450, 2900, and 5800 nm (Table I). For each film thickness, a set of eight samples was prepared under identical conditions so that they would have the same microstructures and composition. Using the techniques described below, one sample was monitored continuously to measure whisker density on the surface and the remaining samples were measured after different periods of time to determine the volume and morphology of the IMC and the stress in the Sn layer.

The amount of Cu–Sn intermetallic compound (Cu_6Sn_5) that formed in each sample was determined using a weighing

method similar to that reported previously [17], [36]. The sample was weighed before and after deposition of each layer to determine the quantity of Sn and Cu deposited initially. After a period of time the sample was etched using a stripping solution (400 g 70% nitric acid, 19 g sulfamic acid, 13 g fluoroboric acid, and 596 g DI water) which selectively removes the Sn layer. The sample was dipped in the stripping solution for 15 seconds and then rinsed twice for 60 seconds each in DI water before drying with compressed nitrogen. Separate studies confirmed that the IMC and Cu layers were unchanged by the Sn etching, suggesting that the rate of stripping IMC and Cu is very slow compare to that of Sn. The sample was weighed before and after selectively etching the unreacted Sn and the change in the sample mass after etching corresponded to the amount of Sn that had not reacted to form IMC; comparison with the initial Sn layer weight enabled us to determine the mass of Sn that had been incorporated into the growing IMC. The mass was converted to an effective IMC thickness per unit area using literature values for the density of the IMC. Measurements were performed at different elapsed times over a 5-day period to quantify the IMC growth kinetics. In addition to the weight change, SEM was used to characterize the interface morphology of the IMC on the surface after the Sn was removed.

The film stress was measured using a wafer curvature technique based on a multi-beam optical system (MOSS) [44], [45]. This approach measures the curvature by monitoring the deflection of an array of initially parallel laser beams with a CCD camera. The average stress in the film can be inferred from the curvature induced in the substrate using an analysis originally described by Stoney [46]. For a complex multilayer film such as used in these studies, the contribution of the different stress in each layer to the curvature must be considered. Approximating each layer as uniform and homogeneous, the measured curvature (1/R) can be approximated by a sum over the average stress $(\langle\sigma\rangle_i)$ and thickness (h_i) of each layer

$$\frac{1}{R} = \frac{6}{M_s h_s^2}[\langle\sigma_{\mathrm{Cu}}\rangle h_{\mathrm{Cu}} + \langle\sigma_{\mathrm{IMC}}\rangle h_{\mathrm{IMC}} + \langle\sigma_{\mathrm{Sn}}\rangle h_{\mathrm{Sn}}].$$

M_S and h_s refer to the biaxial modulus and thickness of the substrate, respectively. The subscript i refers to the different layers in the multilayer (Sn, Cu, and IMC). The average stress in the ith layer is defined as

$$\langle\sigma_i\rangle = \frac{1}{h_i}\int_0^{h_i} \sigma_i(z,t)\,dz.$$

Although the layers are not necessarily homogeneous and uniform, this analysis approximates the actual stress by an effective value for an equivalent uniform layer.

The measured curvature is a composite measurement of the evolving stresses in each of the layers. The stress in the Sn layer can be determined separately from the other layers by measuring the curvature before and after selective etching of the Sn layer (as described above with respect to the weighing measurements). The change in the measured curvature after removal of the Sn corresponds to the value of $\langle\sigma_{\mathrm{Sn}}\rangle h_{\mathrm{Sn}}$Sn assuming that the etching does not affect the stress in the underlying Cu and IMC layers. By stripping different samples at different times, the evolution of the average stress in the Sn layers was obtained.

Whisker growth kinetics are difficult to quantify because the whisker diameter is small (on the order of 1–10 μm) but the spacing between them is relatively large (on the order of 100 μm). Therefore, measurement poses the conflicting needs of high magnification with a large field of view. Scanning electron microscopy is capable of measuring individual whiskers, but obtaining statistics over large numbers is very time consuming. To overcome this, we have developed a technique to monitor the whisker density optically by illuminating the sample at an oblique angle and recording the scattered light with a video camera over a field of view of 1 mm^2. The resolution is insufficient to directly image the shape of surface features under these conditions, but the scattered light is measured as a bright spot. The technique is therefore unable to distinguish between long whiskers and smaller surface protrusions, but it does enable a large area of surface to be monitored continuously over long times and the density of spots to be easily quantified by an image analysis program. We refer to the density of all the measured surface features as "whiskers" even though they do not all have a large aspect ratio. Comparison of the feature density determined by this optical technique with SEM analysis of the same surface confirmed that the two techniques measure the same density. SEM also revealed that slightly more than half of those features were hillocks as opposed to whiskers.

IV. Results

The techniques described above were used to monitor the IMC thickness, stress in the Sn layer and whisker density on three sets of samples with different nominal Sn thicknesses (Table I). The results are shown in Fig. 1 for measurements performed over a period of 5 days for each set of samples.

The IMC volume (Fig. 1(a), (d), (g)) is seen to increase monotonically for all the thicknesses with a rate that decreases with increasing time. The thicker layers have more IMC formation than the thinner layers for the same time period. However, it is important to note that the grain size of the Sn is not the same for the different Sn thicknesses. We determined the grain size from SEM measurements of the surface after the Sn layer was selectively removed by etching (Fig. 2). The bright spots in the image correspond to particles of IMC growing into the Sn layer after nucleating along the Sn grain boundaries at the Sn/Cu interface [17], [21], [42] and [47]. The grain size for each layer thickness is listed in Table I; it increases roughly as the square root of the Sn film thickness, consistent with previous results by Tsuji [9]. Therefore, the observed increase in IMC formation with layer thickness is also correlated with a larger grain size. The morphology of the IMC particles is also revealed in the SEM images after the Sn has been removed. The increase in intermetallic volume with film thickness (or grain size) is accompanied by an increase in the size of the individual particles.

The average stress in the Sn layers is shown in Fig. 1(b), (e), (h). The stress is initially tensile for all three different Sn thicknesses and then becomes increasingly compressive; eventually reaching what appears to be a steady-state compressive stress. In each case, the stress stops changing over time even though the IMC formation

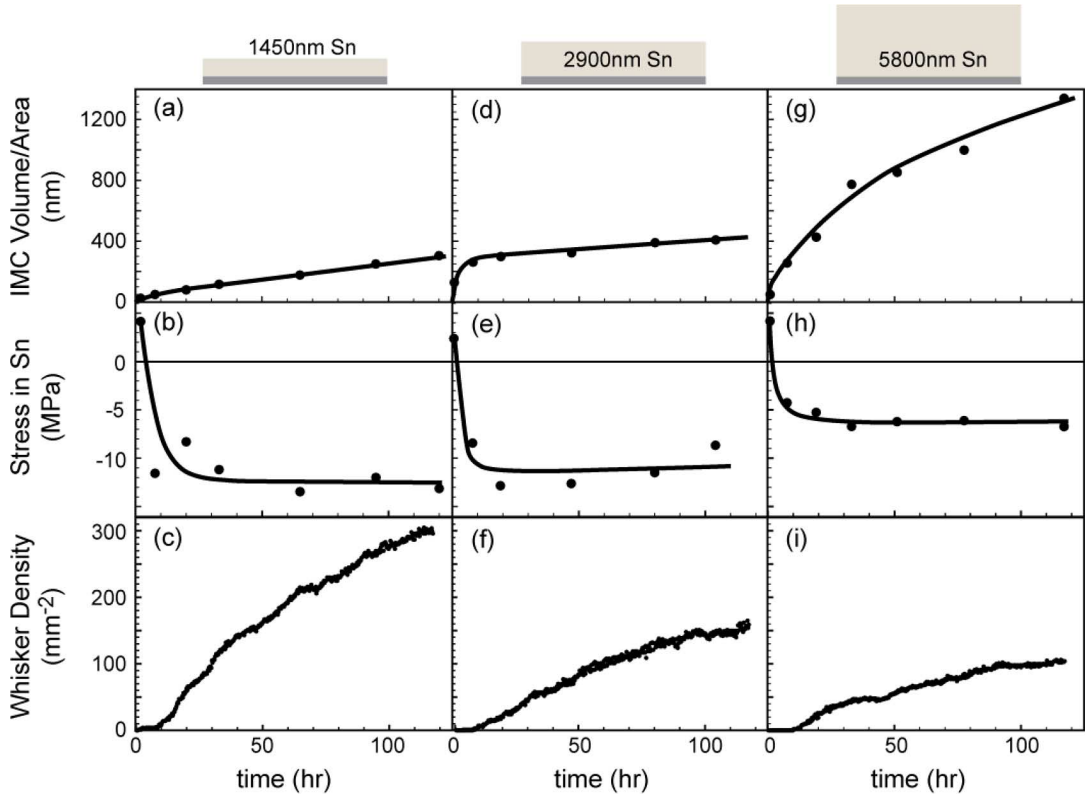

Fig. 1. Measurements of the evolution of IMC volume, Sn stress, and whisker density from samples with Sn thickness of (a)–(c) 1450 nm, (d)–(f) 2900 nm, and (g)–(i) 5800 nm.

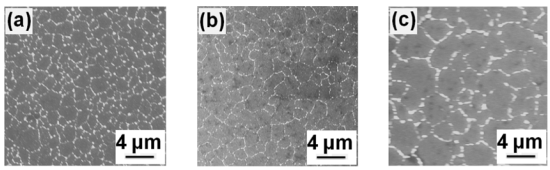

Fig. 2. SEM images of Sn/Cu samples after the Sn layer has been removed by etching. The samples were prepared with initial Sn layer thicknesses of (a) 1450, (b) 2900, and (c) 5800 nm and held for 2–3 hours before etching. The bright spots correspond to particles of IMC.

is observed to continue. Though the nature of the stress evolution is the same for different Sn thickness, the magnitude of the compressive stress is greater for the thinner film. The magnitude of the steady-state stress does not correlate with the amount of intermetallic formed; the thicker samples have less stress even though they have more IMC. As discussed below, we attribute this to a greater degree of stress relaxation in the thicker, larger-grained films.

The corresponding whisker densities [Fig. 1(c), (f), (i)] for each sample are initially small and remain that way for an extended incubation period of 10–15 hours. After that period, the density rapidly increases with a rate that decreases with time. Comparing the different Sn layer thicknesses, we observe more whiskers per unit area for the thinner samples than for the thicker samples. However, if the grain size is taken into account, then the thicker layers have more whiskers per grain than the thin layers. Scaling the area by the grain size indicates that after 5 days the 5800-nm layer has approximately 1 whisker per 1250 grains of Sn while the thinner layers (1450 and 2900 nm) have approximately 1 whisker per 2225 grains.

V. Discussion and Comparison to FEA Simulations

The measurements described in the preceding section clearly indicate correlations between the evolving IMC volume, Sn stress, and whisker density. By comparing the results for the different measured sample thicknesses, we are able to develop insights into the relative importance of different mechanisms. In the section below, we discuss the implications of these measurements in terms of what they suggest about the mechanisms controlling their evolution.

A. Intermetallic Growth Kinetics

Fig. 1 shows that the IMC grows faster in the thicker films (which also have a larger grain size). It is unlikely that the increase in growth rate is caused directly by the increase in film thickness. FIB cross-sectional measurements indicate that the IMC grows primarily outward from the Cu–Sn interface and does not nucleate higher up in the Sn layer, so the particle growth appears to involve processes that occur close to the Sn/Cu interface and therefore would not be expected to depend on the Sn film thickness. It is more likely that the increase in growth rate is a consequence of the increase in grain size that accompanies the increased thickness of the films.

The underlying mechanisms that cause the growth kinetics to depend on grain size are complex, and the influence of grain size on kinetics is difficult to predict. The grain size could influence several processes. Grain boundaries (and in

particular the triple junction between a Sn grain boundary and the underlying Cu film) appear to provide a nucleation site for IMC particles. If particle nucleation were the rate limiting process, however, then reducing the grain size (and so increasing the grain boundary length per unit area) would be expected to increase the IMC growth rate (the opposite of what is seen). A similar argument rules out mass transport along grain boundaries as the rate limiting process. The IMC growth rate appears to increase in proportion to the grain area, which suggests that transport across the Cu/Sn interface may control the IMC growth rate. Cross-section TEM images of evaporated Sn layers [42] show that a fine-grained columnar IMC forms a more uniform layer in the Sn grain interiors in addition to the facetted particles that nucleate at the Sn–Sn grain boundaries. The disparity in size between the particles that form in the Sn grain boundaries and those in the grain interiors indicates there may be a difference in growth rate between the two morphologies, possibly due to a difference in grain orientation. As it thickens, the continuous layer of finer-grained IMC in the grain interiors would be expected to further limit transport. We observe a change in growth kinetics over longer periods of time than those shown in Fig. 1, which is also consistent with a transition from interface-controlled growth at the surface of the faceted particles in the grain boundaries, to diffusion-controlled growth determined by the rate of transport across the thickness of the continuous IMC layer. Ultimately, although we cannot attribute the observed dependence of the growth rate on sample thickness to a simple mechanism, the measurements clearly indicate that the volume of IMC is greater for the thicker, large-grained Sn layers than for the thinner, small-grained layers.

The observation that IMC grows primarily into the Sn layer, rather than the Cu substrate, is consistent with earlier kinetics studies which determined that room temperature growth of Cu_6Sn_5 proceeds at the IMC/Sn interface [35]–[39]. This implies that Cu atoms are the more mobile species, diffusing to the IMC growth front within the Sn layer where they combine with the adjacent Sn atoms to form Cu_6Sn_5. The diffusion of Cu into the Sn leads to a large change in the local volume as the IMC particles grow via the incorporation of Cu. The exact value of the volumetric expansion that results from IMC formation has been the subject of some debate [13], [18], and [43], but if the IMC were to form by insertion of Cu atoms within a pre-existing Sn lattice, the resulting IMC would occupy 44% greater volume than the Sn that it replaces.

The excess volume caused by IMC growth appears to greatly exceed the volume of material that is accommodated within whiskers. For example, if each whisker observed in Fig. 1(c) is assumed to be a single grain, then each whisker would need to be over 350 μm long to accommodate the IMC volume of 300 nm^3/nm^2 measured in Fig. 1(a). In other work on evaporated samples, we estimated the total volume of Sn in the whiskers by counting and measuring directly the whisker length in the SEM; these studies show a total whisker volume of approximately 3 nm^3/nm^2 after 21 days, which is roughly a factor of 500 times smaller than the total IMC volume generated during a comparable period. The remaining IMC volume must be accommodated by some mechanism of deformation within the film. It is this deformation that accounts for the observed stress, as discussed in more detail in the next section.

B. Stress Generation and Relaxation

Understanding how the volume expansion of the growing IMC is accommodated by the surrounding Sn is critical for determining the overall state of stress that develops in the Sn. The magnitude of the volume change is clearly too large to be accommodated by purely elastic deformation of the Sn. In addition, the stress saturates at a relatively low value during the early stages of IMC growth, while the IMC volume continues to increase (see Fig. 1). Stress relaxation processes must therefore prevent the stress from continuing to increase as the IMC continues to grow. The resultant balance between stress generation and stress relaxation determines the magnitude of stress that develops and leads to the saturation seen in Fig. 1.

What are the relaxation processes that control the stress? The growth of whiskers may provide one mechanism for stress relaxation, but several other mechanisms may also play a role. Sn is known to creep rapidly at room temperature [48], both by dislocation creep and grain boundary diffusional creep. Recent TEM analyses also reveal extensive dislocation activity within the Sn, particularly in the vicinity of large IMC grains where dislocations appear to be emitted from the IMC/Sn interface [42] and [47]. The range of dislocation activity extends through the entire thickness of the film; arrays of dislocations are seen to self-organize into sub-grains boundaries and dislocation pileups are observed near the oxide layer.

Stress-driven grain boundary diffusion (Coble creep) is another possible mechanism for relaxing stress. The growth of whiskers with lengths much greater than the film thickness provides clear evidence for long-range transport of Sn [18], [37], [38], and [39]. Further evidence is provided by experiments in which whiskers grow in response to stresses applied far from the root of the whisker, either due to mechanical deformation or growth of IMC [49].

The large-grain boundary diffusivity in Sn suggests that the stress should relax rapidly due to the diffusion of atoms out of the columnar grain boundaries onto the surface. This makes the observation of a steady compressive film stress [Fig. 1(b), (e), (h)] somewhat surprising. A likely explanation for the lack of complete relaxation by Coble creep is that the tenacious Sn surface oxide prevents atoms from diffusing to the surface [38]. Indeed, when the Sn oxide layer is removed by sputtering in vacuum [47] or by chemical etching [48], the stress is seen to rapidly relax. In stress measurements during electrodeposition (where there is no oxide), the stress is also observed to rapidly relax when growth is terminated [50]. This also suggests that the near-columnar grain structure typical of Sn films plays a critical role in preventing stress relaxation by Coble creep. If the film contained a large number of grain boundaries that were oriented parallel to the surface, stress could be relaxed by diffusion of atoms from the columnar boundaries into those oriented parallel to the surface. In practice, there are relatively few such non-columnar boundaries, and those that do exist are often sites for whisker growth [18], [41], [51].

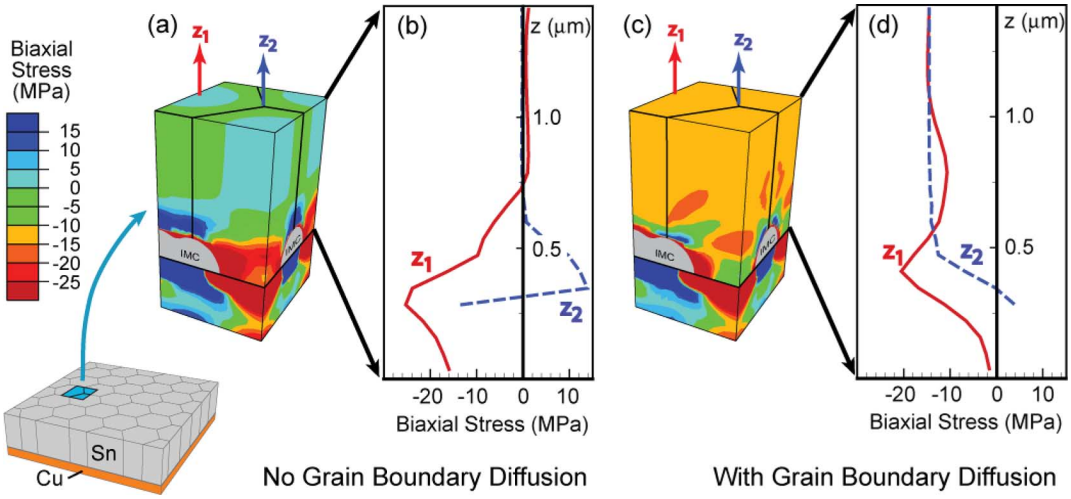

Fig. 3. Results of FEA simulations that predict the evolution of stress in a Sn film with columnar grain structure due to IMC growth. The contour plots (a) and (c) show the three-dimensional distribution of stress through the film; the legend relates the color to the stress state. (b) and (d) show the corresponding stress distributions along the lines Z1 and Z2 indicated on the contour plots. The figures shown in (a) and (b) correspond to a film that relaxes only plastic deformation (i.e., dislocation motion) Sn grains. The results in (c) and (d) correspond to a film that relaxes by both elastic-plastic behavior and grain boundary diffusion in the Sn.

Although diffusion of atoms to the surface appears not to be the principal mechanism for relaxing stress, grain boundary diffusion nevertheless plays an important role in controlling the distribution of stress in the film, in addition to playing a key role in whisker growth. To better understand how dislocation-mediated plastic deformation and stress-driven grain boundary diffusion determine the evolution of stress generated by IMC growth, we have performed a series of finite-element simulations that explicitly model these processes. A full description of the model is presented in [52] so only a brief summary is given here. Our model consists of a periodic array of columnar hexagonal Sn grains with grain size 1.4 μm and thickness 1.5 μm bonded to a Cu substrate (see Fig. 3). The Cu is modeled as an elastic layer with modulus 117 GPa, and the Sn grains are modeled as elastic-perfectly plastic solids with the von Mises yield surface and flow potential (for Sn the modulus is 50 GPa and yield stress is taken as 14.5 MPa [53]. The simulations also account explicitly for stress-driven mass transport in the Sn grain boundaries: grain boundaries are assumed to have a diffusion coefficient 4.8×10^{-9} cm^2/s [54]. We assume there is no flux out of the Sn grain boundaries onto the free surface due to the presence of the Sn-oxide layer. The transformation of Sn to IMC is simulated by applying a localized 44% transformation strain to expanding hemispherical regions at the base of the Sn along the Sn/Sn grain boundaries. Note that our model does not include whisker growth, but is intended to examine the evolution of stress leading up to whisker formation. The numerical simulations allow us to explore the consequences of different assumptions about material behavior in a way that is not possible through experimental measurement alone.

Fig. 3 shows the simulated stress distributions that develop in Sn films that relax by different processes. Fig. 3(a) and (b) shows the stresses in a film in which the grains deform plastically, but no grain boundary diffusion occurs, while Fig. 3(c) and (d) shows the stresses in a film in which both elastic-plastic behavior and grain boundary diffusion can occur. Results are shown for a 1450-nm Sn layer with an IMC volume per area of 170 nm. The contour plots [Fig. 3(a) and (c)] shows the three-dimensional distribution of stress through the film; the relation of the color to the stress state is shown in the legend accompanying the figure. Fig. 3(b) and (d) shows the corresponding stress distributions along the lines Z1 and Z2 indicated on the contour plots.

For the case of plastic deformation with no grain boundary diffusion [Fig. 3(a) and (b)], we find that the stress is limited to the plastically deforming region immediately surrounding the expanding IMC. Immediately above the plastic zone, the stress dies out very rapidly and virtually no stress is transmitted to the upper half of the film. In contrast, when grain boundary diffusion is active [Fig. 3(c) and (d)] the average stress in the Sn quickly reaches a maximum compressive value of approximately -12 MPa, then remains relatively constant throughout the thickness due to the redistribution of volume along the grain boundaries. As a consequence, the majority of the Sn layer is brought to its yield stress. This prediction is consistent with TEM observations that find dislocations across the entire film and even near the surface [42].

Fig. 4 shows the evolution of the average stress in the film calculated by the FEA simulations assuming the different relaxation mechanisms described above. The IMC volume is assumed to increase with a growth rate similar to Fig. 1(a); the corresponding measurement of the average stress is shown by the symbols in the figure. In the case of plastic flow alone (no grain boundary diffusion), the average stress becomes progressively more compressive as the IMC volume increases with time. This gradual increase in average film stress is caused by the increasing penetration of the plastic zone (which is at the yield stress) into the Sn layer. Since the plastic zone is confined to a narrow region near the IMC, the stress averaged through the thickness of the film is small, on the order of a few MPa. When grain boundary diffusion is included, the fraction of the film that is at the yield stress extends over a larger proportion of the total film thickness giving a larger average stress. Moreover, once the film reaches its yield stress no further increase in stress

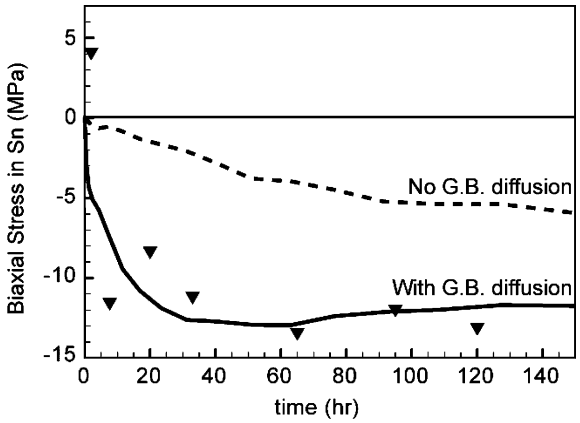

Fig. 4. Comparison between the time variation of the average stress in the Sn layer predicted by FEA simulations and experiment. The dashed line shows FEA predictions for a film that relaxes only by plastic flow in the grain interiors. The solid line shows results for a film that relaxes by both grain boundary diffusion and plastic flow. The symbols represent the corresponding experimental stress measurements (for 1450 nm Sn).

is possible even though the IMC continues to grow. This leads to a saturation of the stress and development of a steady state, similar to what is seen experimentally.

The simulation results suggest that both dislocation-mediated plasticity and grain boundary diffusion play an important role in the stress evolution, making it possible for stress to spread across the Sn layer and saturate with relatively small amounts of IMC growth. The combination of these mechanisms alone, however, cannot explain the differences in stress level measured for different thickness Sn samples. Our FEA models predict very similar stress levels for films ranging in thickness from 1.5 μm to 9 μm. The smaller steady-state stress for the thicker, large-grained films therefore suggests that stress relaxation within the Sn grains is enhanced for these samples. Such an increase in stress relaxation with film thickness (or grain size) may be due to a lower yield stress or, alternatively, an enhancement of creep relaxation with grain size (as seen experimentally [48]).

C. Whisker Nucleation and Growth

The onset of whisker nucleation [Fig. 1(g)–(i)] correlates directly with the observed buildup of compressive stress. We see an incubation period of several hours for each sample before the whiskers start to form, which coincides with the saturation of the stress in the Sn layer. Whiskers are only observed to start growing after the stress in the Sn reaches its steady-state compressive value. The correlation of the whisker nucleation with the stress is a further indication that stress is the driving force for whiskers to form, and also suggests that whiskers do not nucleate until the other stress relaxation mechanisms have spread the stress through the full thickness of the Sn layer.

The steady-state stress in the thick Sn films is lower than in the thin samples, but it is not immediately clear how this is related to the nucleation kinetics. At first sight, the raw data in Fig. 1(c), (f), and (i) suggests that thinner films are more prone to whisker nucleation than the thicker films since the number of whiskers per unit area is higher. However, whiskers generally either consist of a single grain that progressively extends from the film surface, or a group of grains which protrude together to form a hillock. Scaling the areal density by the grain size suggests that a larger fraction of grains develop whiskers in the thickest film (recall that the whisker density data include whiskers as well as hillocks).

Although there is a clear correlation between the evolution of stress in the Sn and whisker nucleation, our experiments alone do not directly reveal the mechanisms responsible for whisker nucleation and growth. Furthermore, we cannot tell from the data if the lower stress in the thick films is due to greater relaxation by plastic flow processes or due to the onset of whisker growth. To provide some insight into the coupling between stress generation, relaxation, and whisker growth, we have extended the finite-element simulations described in the preceding section to account for the growth of whiskers [55]. In particular, we address the questions of how stress relaxation is partitioned between whisker growth and plastic flow processes, as well as how whisker growth can be sustained despite the low driving force. To achieve sufficient driving force, previous models of whisker growth due to stress-driven diffusion require either background stress levels [39] or whisker densities [51] significantly greater than those measured here.

As described in the preceding section, our simulations model a polycrystalline film with columnar microstructure (see Fig. 3). For simplicity, IMC growth is approximated by applying a uniform volumetric expansion at a steady rate (de/dt) in all the grains. The film can accommodate this strain by a combination of plastic flow within individual grains and stress-driven diffusion of material along grain boundaries. We provide an additional mechanism for whisker growth by adding a periodic distribution of "soft" grains, whose yield stress is lower than that of the other grains. Stress gradients form around the soft grains which drive grain boundary diffusion. Strain is then relaxed as the soft grain accumulates new material and is extruded from the surface of the film. A similar process would be observed for a grain that contains a non-columnar grain boundary: the key feature that leads to whisker growth is that a few grains in the microstructure are able to relax stress more effectively than their near neighbors.

A representative result is shown in Fig. 5. The contours show distributions of effective plastic strain around the whisker. The soft grain deforms plastically, and is extruded from the film. The lower stress in the whiskered grain relaxes its neighbors, and leads to a stress gradient that drives diffusion towards the whisker. Because of the enhanced relaxation, the grains surrounding the whisker remain elastic, but far from the whisker, continued IMC growth causes all the grains to deform plastically. In the outer region, the film accommodates the IMC volume by a uniform plastic strain that causes the film to thicken, while in the inner region the excess volume is accommodated by flow of material into the whisker. An important consequence of accounting for the continual generation of strain by IMC growth is that the balance between the rate of volume production and material transport to the whisker determines the radius of the diffusion field surrounding the whisker. As the IMC growth rate is reduced the size of the relaxed region around the whisker increases. For sufficiently low IMC growth rates and sufficiently high whisker densities

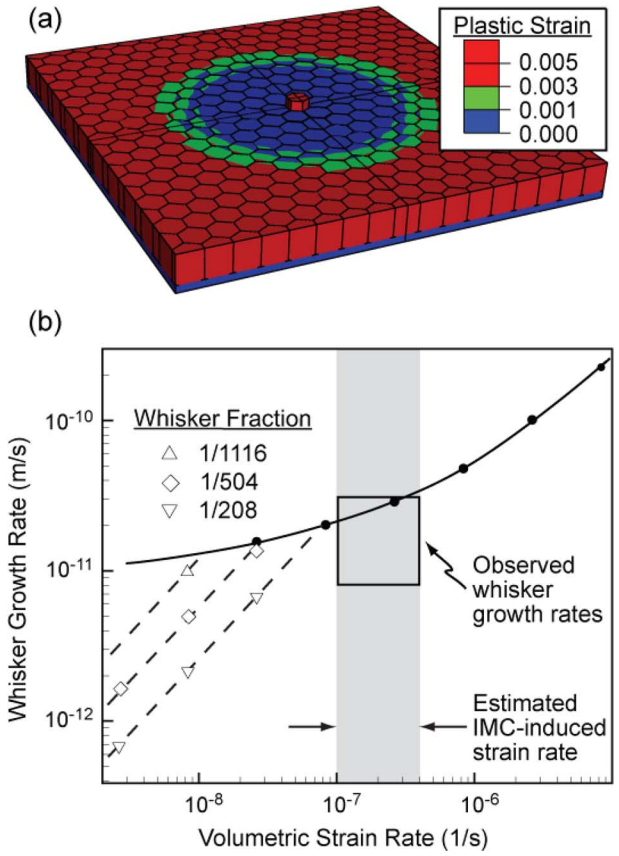

Fig. 5. Results of FEA model of stress evolution and whisker growth in a Sn film. (a) Distribution of equivalent plastic strain surrounding a whisker grain during steady-state growth. The periodic cell surrounding a single whisker is shown. The total volumetric strain is 0.25%, and the applied volumetric strain rate is 8.3×10^{-7}/s. (b) Predicted steady-state whisker growth rate as a function of volumetric strain rate due to IMC formation. The solid curve shows the growth rate when whisker density is low enough that neighboring whiskers do not interact. The whisker grains are assumed to support 0.2 times the yield stress of the surrounding grains. Dashed lines show the growth rate when the diffusion fields of neighboring whiskers overlap; symbols indicate associated density of "soft" grains.

the radius of the diffusion field may become comparable to the whisker spacing. At this point, the film is fully relaxed by whisker growth, and plastic flow is negligible.

The predicted whisker growth rate (shown as the rate of change of whisker height) is plotted as a function of volumetric strain rate due to IMC growth in Fig. 5(b). The figure shows two regimes of behavior. The solid curve shows the whisker growth rate when whisker density is low enough that whiskers do not interact. In this regime, each whisker relaxes only a limited region surrounding itself as shown in Fig. 5(a) and the average stress in the film is controlled primarily by plastic flow processes. The series of dashed lines in Fig. 5(b) show whisker growth rates that result when whisker density is high enough that the size of the relaxed region around the whiskers becomes comparable to their spacing. In this regime, the film is fully relaxed by whisker growth, and the whisker growth rate is proportional to the IMC growth. Each dashed line corresponds to a different whisker density, expressed as fraction of whiskers grains per Sn grain. Note that the greatest fractional density of whiskers observed in our experiments is 1 whisker per 1250 grains, which would plot to the left of the line corresponding to one whisker per 1116 grains in Fig. 5(b).

Comparison of our model predictions with experiment requires an estimate of the volumetric strain rate produced by IMC growth. An upper bound value can be determined by assuming that all excess volume generated by IMC growth contributes to the volumetric strain in the Sn. For the IMC growth rates presented in Fig. 1, the corresponding volumetric strain rates range from 1×10^{-7}/s to 4×10^{-7}/s and are indicated by the shaded region in Fig. 5(b). The boxed region in Fig. 5(b) shows the range of whisker growth rates determined by our own SEM measurements of whisker growth over time as well as values reported in the literature [39], [43]. As shown in Fig. 5(b), the predicted whisker growth rates are in relatively good agreement with the range of experimental measurements. The comparison also indicates that for typical whisker densities and IMC growth rates, plastic flow is likely the dominant mechanism of stress relaxation.

D. Implications for Mitigation

Our measurements and computational models provide some insight into the effectiveness of potential strategies to mitigate whisker formation. One possible approach is to lower the rate of IMC growth. Commonly used processes such as reflow and annealing create a more uniform IMC layer that decreases the subsequent amount of IMC that forms after the initial processing. IMC growth can also be inhibited by the use of diffusion-barriers such as Ni to prevent Cu–Sn IMC formation [30]. However, this is only a kinetic barrier and does not remove the driving force for IMC formation, so if the barrier is disrupted (e.g., by mechanical deformation or thermal cycling) then whisker formation can occur again. In addition, our experiments and FEA simulations suggest that whisker growth rates are relatively insensitive to IMC growth rate, unless the growth rate is reduced sufficiently to ensure that whiskers are the dominant relaxation mechanism in the film. Such low IMC growth rates may be difficult to achieve in practice. Another possible way to reduce whiskering would be to lower the background stress level, thus reducing the stress gradients that drive material to diffuse to the whiskers. This could be done by enhancing stress relaxation, for example by weakening the surface oxide and enabling the stress to relax by diffusion of atoms to the surface. Paradoxically, similar results could be obtained by greatly increasing the fraction of "weak" (low stress) grains which lead to whiskers. If the film consists predominantly of weak grains, they will relax the stress, but without forming whiskers. This is consistent with the suppression of whiskering in Pb–Sn layers, where the presence of a more equiaxed microstructure with abundant oblique grain boundaries also enhances the rate of stress relaxation via Coble creep [18], [48]. Sn–Bi [56] and other alloy additions [57] have also been investigated as a means to modify the microstructure and enhance stress relaxation in the Sn layer.

VI. Conclusion

Experiments and FEA simulations have been used to investigate the influence of IMC growth, microstructure, and stress relaxation mechanisms on whisker evolution in Sn films. By measuring the IMC volume, stress and whisker nucleation and

growth kinetics simultaneously on films of different Sn thickness (and grain size), we have quantified the correlations between these parameters for comparison with different mechanisms. We recognize that the observed steady-state stress in the Sn results from a balance between stress generation (local volume expansion associated with IMC growth) and stress relaxation mechanisms (dislocation-mediated plasticity or creep, stress-driven grain boundary diffusion, whisker growth). Numerical simulations of stress evolution show that the combination of plastic deformation within Sn grains and diffusion along grain boundaries is sufficient to produce the observed time evolution of average stress. An FEA model relates the whisker growth rate to the IMC-induced strain rate in the Sn; depending on the whisker density, the strain from the IMC can be accommodated by the growth of whiskers or by other relaxation processes. For typical whisker densities observed experimentally, the model indicates that stress is not relaxed primarily by whisker growth. This suggests that the "background" steady-state stress is maintained by the balance of IMC growth and internal deformation within the film. Where whiskers emerge, their subsequent growth provides additional relaxation within their local neighborhood. Specifically, we expect a stress gradient to develop radially and vertically around the whisker root to drive transport of material towards the whisker. This gradient would appear as a perturbation superimposed on the more uniform background stress field; strain gradients around whiskers have been experimentally confirmed [19], [34].

ACKNOWLEDGMENT

The authors would like to thank J. W. Shin, W. L. Chan, and G. Barr for their helpful contributions.

REFERENCES

[1] Multiple Examples of Whisker-Induced Failures are Documented on the NASA Website [Online]. Available: http://nepp.nasa.gov/whisker/

[2] F. C. Frank, "On tin whiskers," *Philosophical Mag.*, vol. 44, p. 851, 1953.

[3] S. M. Arnold, "Growth of metal whiskers on electrical components," in *Proc. Elect. Compon. Conf.*, 1959, pp. 75–82.

[4] K. G. Compton, A. Mendizza, and S. M. Arnold, "Filamentary growths on metal surfaces—Whiskers," *Corrosion*, vol. 7, p. 327, 1951.

[5] G. T. Galyon, "Annotated tin whisker bibliography and anthology," *IEEE Trans. Elect. Packag. Manuf.*, vol. 28, no. 1, pp. 94–122, Jan. 2005.

[6] V. K. Glazunova, "A study of the influence of certain factors on the growth of filamentary tin crystals," *Translated From Kristallografiya*, vol. 7, no. 5, pp. 761–768, 1962.

[7] W. C. Ellis, D. F. Gibbons, and R. C. Treuting, "Growth of metal whiskers from the solid," in *Growth and Perfection of Crystals*, R. H. Doremus, B. W. Roberts, and D. Turnbull, Eds. New York: Wiley, 1958, pp. 102–120.

[8] B. D. Dunn, "A laboratory study of tin whisker growth," *Eur. Space Agency (ESA) Rep. STR-223*, pp. 1–51, 1987.

[9] K. Tsuji, "Role of grain boundary free energy & surface free energy for tin whisker growth," in *Proc. IPC-JEDEC Conf.*, Frankfurt, Germany, 2003, pp. 169–186.

[10] I. Boguslavsky and P. Bush, "Recrystallization principles applied to whisker growth in tin," in *Proc. 2003 APEX Conf.*, Anaheim, CA, 2003, pp. S12-4-1–S12-4-10.

[11] J. D. Eshelby, "A tentative theory of metallic whisker growth," *Phys. Rev.*, vol. 91, pp. 755–756, 1953.

[12] M. W. Barsoum, E. N. Hoffman, R. D. Doherty, S. Gupta, and A. Zavaliangos, "Driving force and mechanism for spontaneous metal whisker formation," *Phys. Rev. Let.*, vol. 93, p. 206104-1, 2004.

[13] B. Z. Lee and D. N. Lee, "Spontaneous growth mechanism of tin whiskers," *Acta Metallurgica*, vol. 46, no. 10, pp. 3701–3714, 1998.

[14] K. N. Tu, "Interdiffusion and reaction in bimetallic Cu-Sn thin films," *Acta Metallurgica*, vol. 21, no. 4, pp. 347–354, 1973.

[15] C. Xu, Y. Zhang, C. Fan, and J. A. Abys, "Driving force for the formation of Sn whiskers: Compressive stress—Pathways for its generation and remedies for its elimination and minimization," *IEEE Trans. Elect. Packag. Manuf.*, vol. 28, no. 1, pp. 31–35, Jan. 2005.

[16] U. Lindborg, "Observations on the growth of whisker crystals from zinc electroplate," *Metallurgical Trans. A*, vol. 6A, pp. 1581–1586, 1975.

[17] W. Zhang, A. Egli, F. Schwager, and N. Brown, "Investigation of Sn–Cu intermetallic compounds by AFM: New aspects of the role of intermetallic compounds in whisker formation," *IEEE Trans. Elect. Packag. Manuf.*, vol. 28, no. 1, pp. 85–93, Jan. 2005.

[18] W. J. Boettinger, C. E. Johnson, L. A. Bendersky, K.-W. Moon, M. E. Williams, and G. R. Stafford, "Whisker and hillock formation on Sn, Sn–Cu and Sn–Pb electrodeposits," *Acta Mater.*, vol. 53, no. 19, pp. 5033–5050, Nov. 2005.

[19] W. J. Choi, T. Y. Lee, K. N. Tu, N. Tamura, R. S. Celestre, A. A. MacDowell, Y. Y. Bong, and L. Nguyen, "Tin whiskers studied by synchrotron radiation scanning X-ray micro-diffraction," *Acta Mater.*, vol. 51, pp. 6253–6261, 2003.

[20] C. Xu, Y. Zhang, C. Fan, J. Abys, L. Hopkins, and F. Stevie, "Understanding whisker phenomenon: Driving forces for the whisker formation," in *Proc. IPC SMEMA APEX Conf.*, 2002, pp. S 06-2-1–S 06-2-6.

[21] G. T. T. Sheng, C. F. Hu, W. J. Choi, K. N. Tu, Y. Y. Bong, and L. Nguyen, "Tin whiskers studied by focused ion beam imaging and transmission electron microscopy," *J. Appl. Phys.*, vol. 92, no. 1, pp. 64–69, 2002.

[22] R. M. Fisher, L. S. Darken, and K. G. Carroll, "Accelerated growth of tin whiskers," *Acta Metallurgica*, vol. 2, no. 3, pp. 368–372, May 1954.

[23] S.-K. Lin, Y. Yorikado, J. Jiang, K.-S. Kim, K. Suganuma, S.-W. Chenb, M. Tsujimoto, and I. Yanada, "Mechanical deformation-induced Sn whiskers growth on electroplated films in the advanced flexible electronic packaging," *J. Mater. Res.*, pp. 1975–1986, 2007.

[24] T. Shibutani, Q. Yu, M. Shiratori, and M. G. Pecht, "Pressure-induced tin whisker formation," *Microelectron. Rel.*, vol. 48, pp. 1033–1039, 2008.

[25] R. R. Hasiguti, "A tentative explanation of the accelerated growth of tin whiskers," *Acta Metallurgica (Letters to the Editor)*, vol. 3, no. 2, pp. 200–201, 1955.

[26] C. Xu, Y. Zhang, C. Fan, and J. Abys, "Understanding whisker phenomenon: The driving force for whisker formation," *Circuit Tree Mag.*, pp. 94–105, Apr. 2002.

[27] M. E. Williams, C. E. Johnson, K. W. Moon, G. R. Stafford, C. A. Handwerker, and W. J. Boettinger, "Whisker formation on electroplated SnCu," in *Proc. AESF SUR/FIN Conf.*, 2002, pp. 31–39.

[28] K. N. Tu and K. Zeng, "Reliability issues of Pb-free solder joints in electronic packaging technology," in *Proc. IEEE Elect. Compon. Technol. Conf.*, 2002, pp. 1194–1199.

[29] J. Chang-Bing Lee, Y.-L. Yao, F.-Y. Chiang, P. J. Zheng, C. C. Liao, and Y. S. Chou, "Characterization study of lead-free SnCu plated packages," in *Proc. IEEE Elect. Compon. Technol. Conf.*, 2002, pp. 1238–1245.

[30] Y. Zhang, C. Xu, C. Fan, J. Abys, and A. Vysotskaya, "Understanding whisker phenomenon: Whisker index and tin/copper, tin/nickel interface," in *Proc. IPC SMEMA APEX Conf.*, 2002, pp. S061-1–S06-1-10.

[31] Y. Zhang, C. Fan, C. Xu, O. Khaselev, and J. A. Abys, "Tin whisker growth—Substrate effect understanding CTE mismatch and IMC formation," *IPC Printed Circuits Expo, SMEMA Council APEX Designers Summit*, 2004.

[32] G. T. Galyon and L. Palmer, "An integrated theory of whisker formation: The physical metallurgy of whisker formation and the role of internal stresses," *IEEE Trans. Elect. Packag. Manuf.*, vol. 28, no. 1, pp. 17–30, Jan. 2005.

[33] M. Sobiech, U. Welzel, E. J. Mittemeijer, W. Hügel, and A. Seekamp, "Driving force for Sn whisker growth in the system Cu–Sn," *Appl. Phys. Lett.*, vol. 93, pp. 011906-1–011606-3, 2008.

[34] M. Sobiech, M. Wohlschlögel, U. Welzel, E. J. Mittemeijer, W. Hügel, A. Seekamp, W. Liu, and G. E. Ice, "Local, submicron, strain gradients as the cause of Sn whisker growth," *Appl. Phys. Lett.*, vol. 94, pp. 221901-1–221901-3, 2009.

[35] K. N. Tu and R. D. Thompson, "Kinetics of interfacial reaction in bimetallic Cu–Sn thin films," *Acta Metallurgica*, vol. 30, pp. 947–952, 1982.

[36] P. Oberndorff, M. Dittes, and L. Petit, "Intermetallic formation in relation to tin whiskers," in *Proc. IPC/Soldertec Int. Conf. Lead-Free Electronics "Towards Implementation of the RHS Directive*, Brussels, Belgium, Jun. 11–12, 2003, pp. 170–178.

[37] B. Hutchinson, J. Oliver, M. Nylen, and J. Hagstrom, "Whisker growth from tin coatings," *Mater. Sci. Forum*, vol. 40, pp. 465–470, 2004.
[38] T. A. Woodrow, "Tracer diffusion in whisker-prone tin platings," in *Proc. SMTA Int. Conf.*, Sep. 24–28, 2006.
[39] K. N. Tu, "Irreversible processes of spontaneous whisker growth in bimetallic Cu–Sn thin film reactions," *Phys. Rev. B*, vol. 49, pp. 2030–2034, 1994.
[40] K. N. Tu, C. Chen, and A. T. Wu, "Stress analysis of spontaneous Sn whisker growth," *J. Mater. Sci.: Mater. Electron.*, vol. 18, pp. 269–281, 2007.
[41] J. Smetana, "Theory of tin whisker growth: "The end game"," *IEEE Trans. Elect. Packag. Manuf.*, vol. 30, no. 1, pp. 11–22, Jan. 2007.
[42] K. S. Kumar, L. Reinbold, A. F. Bower, and E. Chason, "Plastic deformation processes in Cu/Sn bimetallic films," *J. Mater. Res.*, pp. 2916–2934, 2008.
[43] M. Dittes, P. Oberndorff, and L. Petit, "Tin whisker formation—Results, test methods and countermeasure," in *Proc. IEEE Elect. Compon. Technol. Conf.*, 2003, pp. 822–826.
[44] E. Chason and J. A. Floro, "Measurements of stress evolution during thin film growth," in *Proc. Mater. Res. Symp.*, 1996, vol. 428, p. 499.
[45] J. A. Floro, E. Chason, S. R. Lee, R. D. Twesten, R. Q. Hwang, and L. B. Freund, "Real-time stress evolution during Si1-xGex heteroepitaxy: Dislocations, islanding, and segregation," *J. Elect. Mater.*, vol. 26, no. 9, 1997.
[46] L. B. Freund and S. Suresh, *Thin Films Materials: Stress, Defect Formation and Surface Evolution*, 1st ed. Cambridge, U.K.: Cambridge Univ. Press, 2009, pp. 86–93.
[47] E. Chason, N. Jadhav, W. L. Chan, L. Reinbold, and K. S. Kumar, "Whisker formation in Sn and Pb–Sn coatings: Role of intermetallic growth, stress evolution and plastic deformation processes," *Appl. Phys. Lett.*, vol. 92, pp. 171901-1–17901-3, 2008.
[48] J. W. Shin and E. Chason, "Stress behavior of electroplated Sn films during thermal cycling," *J. Mater. Res.*, vol. 24, pp. 1522–1528, 2009.
[49] L. Reinbold, N. Jadhav, E. Chason, and K. S. Kumar, "Relation of Sn whisker formation to intermetallic growth: Results from a novel Sn–Cu "bimetal ledge specimen"," *J. Mater. Res.*, vol. 24, pp. 3583–3589, 2009.
[50] J. W. Shin and E. Chason, "Compressive stress generation in Sn thin films and the role of grain boundary diffusion," *Phys. Rev. Lett.*, vol. 103, pp. 056102-1–056102-4.
[51] Y. Nakadaira, S. Jeong, J. Shim, J. Seo, S. Min, T. Cho, S. Kang, and S. Oh, "Growth of tin whiskers for lead-free plated leadframe packages," *Microelectron. Rel.*, vol. 47, pp. 1928–1949, 2007, in high humid environments and during thermal cycling.
[52] E. Buchovecky, N. Jadhav, A. F. Bower, and E. Chason, "Finite element modeling of stress evolution in Sn films due to growth of Cu_6Sn_5 intermetallic," *J. Elec. Mater.*, vol. 38, pp. 2676–2684.
[53] W. F. Gale and T. C. Totemeier, *Smithells Metals Reference Book*, 8th ed. New York: Elsevier Butterworth-Heinemann, 2004, pp. 22–96.
[54] W. Lange and D. Bergner, "Messung der Korngrenzenselbstdiffusion in polykristallinem Zinn," *Phys. Statist. Sol.*, vol. 2, pp. 1410–1414, 1962.
[55] E. J. Buchovecky, N. Du, and A. F. Bower, "A model of Sn whisker growth by coupled plastic flow and grain boundary diffusion," *Appl. Phys. Lett.*, vol. 94, pp. 191904-1–191904-3, 2009.
[56] E. Sandnes, M. E. Williams, M. D. Vaudin, and G. R. Stafford G.R., "Equi-axed grain formation in electrodeposited Sn-Bi," *J. Elect. Mater.*, vol. 37, no. 4, pp. 490–497, Apr. 2008.
[57] A. Rae and C. A. Handwerker, "NEMI's characterization of lead-free alloy applicable to today's commercially available alloys," *Circuits Assembly*, vol. 15, no. 4, pp. 20–25, Apr. 2004.

Nitin Jadhav, photograph and biography not available at the time of publication

Eric J. Buchovecky, photograph and biography not available at the time of publication

Lucine Reinbold, photograph and biography not available at the time of publication

Sharvan Kumar, photograph and biography not available at the time of publication

Allan F. Bower, photograph and biography not available at the time of publication

Eric Chason, photograph and biography not available at the time of publication